

The TBK1 adaptor and autophagy receptor NDP52 restricts the proliferation of ubiquitin-coated bacteria

Teresa L M Thurston^{1,3}, Grigory Ryzhakov¹⁻³, Stuart Bloor^{1,3}, Natalia von Muhlinen¹ & Felix Randow¹

Cell-autonomous innate immune responses against bacteria attempting to colonize the cytosol of mammalian cells are incompletely understood. Polyubiquitylated proteins can accumulate on the surface of such bacteria, and bacterial growth is restricted by Tank-binding kinase (TBK1). Here we show that NDP52, not previously known to contribute to innate immunity, recognizes ubiquitin-coated *Salmonella enterica* in human cells and, by binding the adaptor proteins Nap1 and Sintbad, recruits TBK1. Knockdown of NDP52 and TBK1 facilitated bacterial proliferation and increased the number of cells containing ubiquitin-coated salmonella. NDP52 also recruited LC3, an autophagosomal marker, and knockdown of NDP52 impaired autophagy of salmonella. We conclude that human cells utilize the ubiquitin system and NDP52 to activate autophagy against bacteria attempting to colonize their cytosol.

Salmonella enterica is a Gram-negative bacterium that includes serotypes highly pathogenic for humans. Its serovars Typhi and Typhimurium cause typhoid fever and severe gastroenteritis, respectively, and together claim more than 3 million lives annually¹. Upon infection, *Salmonella enterica* Typhimurium (hereafter, *S. Typhimurium*) invades epithelial cells, where it thrives in vesicles dubbed 'salmonella-containing vacuoles' (SCV). SCVs interact transiently with early endosomes, before they acidify and acquire late endosomal markers such as LAMP1 (ref. 2). *S. Typhimurium* regulates SCV maturation through effector proteins injected by type III secretion systems into the mammalian cytosol³. However, some bacteria are nevertheless released from SCVs into the cytosol. Cell-autonomous innate immunity against such cytosolic bacteria is poorly understood. However, because a dense layer of polyubiquitylated proteins can accumulate around cytosolic bacteria⁴, the invasion of the mammalian cytosol by *S. Typhimurium* clearly does not go unnoticed. This ubiquitin coat has been detected *in situ* with antibodies specific for conjugated ubiquitin, but it remains to be seen whether the bacterial surface itself is ubiquitylated or whether ubiquitylated host proteins accumulate around the bacterium. The biological consequences of ubiquitylation are often determined by the type of linkage that connects ubiquitin subunits in a ubiquitin chain, but for the bacterial ubiquitin coat neither has this information been obtained nor has the identity of the E3 ubiquitin ligase(s) responsible been found. Notably, compared to wild-type cells, cells deficient in Tank-binding kinase (TBK1; A001597) harbor more *S. Typhimurium* outside SCVs and fail to restrict bacterial proliferation⁵. TBK1, a noncanonical member of the inhibitor of nuclear factor κ B kinase (IKK) family, has been suggested to control the integrity of SCVs by limiting the expression of the water channel aquaporin-1 (ref. 6). Enhanced amounts

of aquaporin-1 were proposed to impair the cellular response to bacterially induced membrane damage and to favor bacterial proliferation⁶. The homeostatic function of TBK1 in regulating aquaporin-1 expression contrasts with its role in innate antiviral immunity, where, upon viral infection, TBK1 activity is required to induce expression of genes encoding type 1 interferons and other antiviral proteins⁷⁻¹⁰. It therefore seems likely that TBK1 may also function downstream of bacterial detection.

The NF- κ B-controlling canonical IKK complex consists of two TBK1-related kinases, IKK α and IKK β , and a regulatory subunit called NEMO. Activation of the IKK complex requires NEMO to bind ubiquitin chains. These chains were originally thought to consist of Lys63-linked ubiquitins but more recently NEMO was shown to bind preferentially to Met1-linked (also called linear) diubiquitin¹¹⁻¹⁵. Considering the well established role of ubiquitin in regulating the canonical IKK complex, and that *S. Typhimurium* becomes poly-ubiquitin coated if released from SCVs^{4,5,16}, we wondered whether TBK1 may act downstream of the detection of such ubiquitin-coated bacteria.

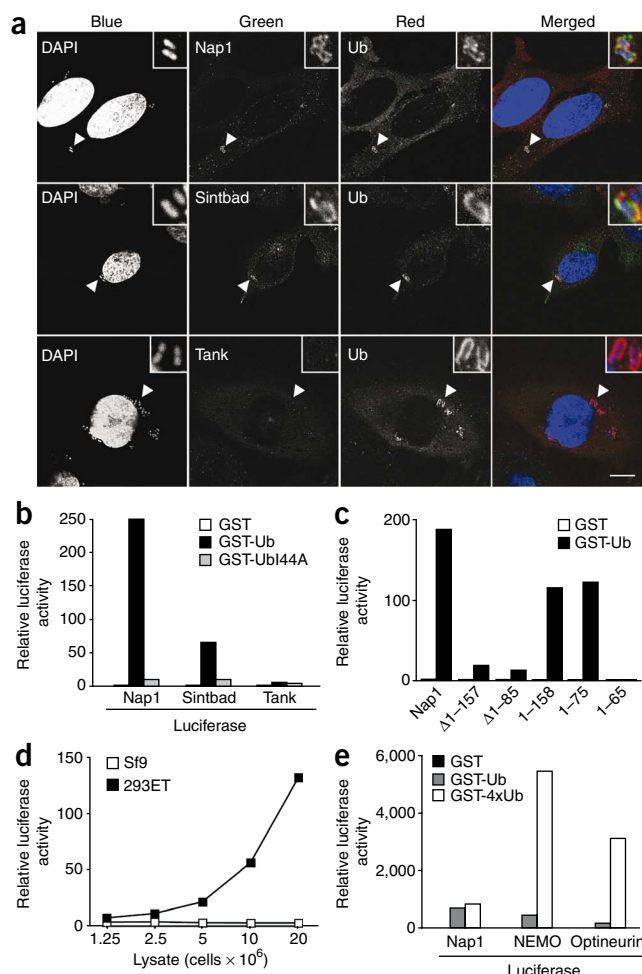
RESULTS

Nap1 and Sintbad bind ubiquitin indirectly

The adaptor proteins Tank, Nap1 and Sintbad (also known as TBKBP) link TBK1 to upstream signaling events¹⁷⁻²⁰. Knockdown experiments have shown these adaptors to be required for antiviral signaling, but their precise molecular function is unknown²⁰⁻²³. We therefore tested whether *S. Typhimurium* that had escaped from SCVs and had become coated with ubiquitin would recruit any of the TBK1 adaptors. Upon infection of HeLa cells with wild-type *S. Typhimurium*, a fraction of bacteria stained positive for ubiquitin, as had been

¹Medical Research Council Laboratory of Molecular Biology, Division of Protein and Nucleic Acid Chemistry, Cambridge, UK. ²Present address: Kennedy Institute of Rheumatology, Imperial College London, London, UK. ³These authors contributed equally to this work. Correspondence should be addressed to F.R. (randow@mrc-lmb.cam.ac.uk).

Received 6 July; accepted 9 September; published online 11 October 2009; doi:10.1038/ni.1800



reported before⁴, and those bacteria were also positive for Nap1 and Sintbad but not Tank (Fig. 1a). To address whether this colocalization of Nap1 and Sintbad with ubiquitin-coated bacteria was due to the adaptors binding ubiquitin, we performed luminescence-based mammalian interactome mapping (LUMIER) assays^{13,24}, which measure the binding between luciferase-tagged prey proteins (here, adaptors) and bait proteins (here, ubiquitin) fused to tags amenable to affinity purification (here, glutathione S-transferase (GST)) (Fig. 1b and Supplementary Fig. 1). Nap1 and Sintbad but not Tank bound ubiquitin. This interaction required the canonical binding surface of ubiquitin, as ubiquitin I44A bound neither Nap1 nor Sintbad. Deletion mutants of Nap1 demonstrated that ubiquitin binding required the amino-terminal domain of Nap1 (Fig. 1c). This domain is conserved between Nap1 and Sintbad but is absent from Tank²⁰, consistent with the observed ability or inability of these adaptor proteins to bind ubiquitin.

The binding of ubiquitin to the Nap1 fragment consisting of amino acids 1–75 was observed when the Nap1 fragment was extracted from human 293ET (Fig. 1c) cells but not when the same Nap1 fragment was expressed in *Escherichia coli* (Fig. 1d), suggesting that the interaction between Nap1 and ubiquitin might be indirect and mediated by a third protein not present in bacteria. Indeed, we found that the addition of lysates from human 293ET but not from insect Sf9 cells restored binding of the bacterially expressed Nap1 fragment to ubiquitin (Fig. 1d); these results demonstrate that human but not insect or bacterial cells contain a factor required for the formation of Nap1–ubiquitin complexes. Two well known ubiquitin-binding

Figure 1 The TBK1 adaptor Nap1 is recruited to ubiquitin-coated *S. Typhimurium* and binds ubiquitin indirectly. (a) Confocal micrographs of HeLa cells expressing yellow fluorescent protein (YFP) fused to Nap1, Sintbad or Tank and infected with *S. Typhimurium*, stained for ubiquitin (Ub) 2 h after infection. At least 100 cells were analyzed. DAPI, 4,6-diamidino-2-phenylindole. Scale bar, 10 μ m; arrowheads, bacteria shown in insets. (b–e) Normalized ratio between luciferase activity bound to beads and present in lysates. The indicated purified GST fusion proteins coupled to beads were incubated with lysates of 293ET cells expressing Nap1, Sintbad or Tank, each fused to luciferase (b), lysates of 293ET cells expressing the indicated Nap1 mutants fused to luciferase (c), lysates of *E. coli* expressing Nap1(1–85) fused to luciferase (d), and lysates of 293ET cells expressing Nap1, NEMO or Optineurin fused to luciferase (e). The reaction in d was complemented with lysates of 293ET and Sf9 cells obtained from the indicated number of cells. Fusion proteins are further characterized in Supplementary Figure 1. All data are representative of at least two independent experiments.

proteins, NEMO and Optineurin, have recently been found to be associated with Tank and TBK1 respectively^{25,26}. However, as NEMO and Optineurin preferentially bound tetraubiquitin chains, they are distinct from the factor that mediates the formation of Nap1–ubiquitin complexes (Fig. 1e).

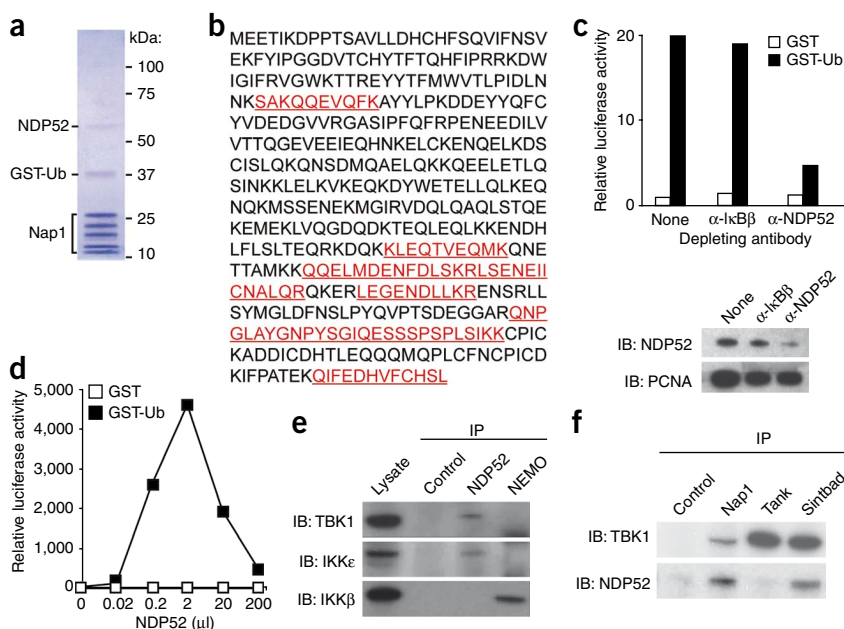
NDP52 bridges ubiquitin and TBK1 complexes

To identify this unknown ubiquitin-binding component of TBK1 complexes, we fractionated HeLa cell extracts according to the scheme shown in Supplementary Figure 2. The final eluate contained, besides remnants of the affinity ligands Nap1 and ubiquitin, a protein that we identified as NDP52 (nuclear dot protein 52 kDa) by mass spectrometry (Fig. 2a,b). NDP52, originally suggested to be a component of nuclear promyelocytic leukemia bodies²⁷, is a mainly cytosolic protein²⁸ that binds to myosin VI (ref. 29) but does not, to our knowledge, have a recognized role in immunity. NDP52 was expressed in all tissues tested (Supplementary Fig. 3). It comprises an N-terminal SKICH domain³⁰, a coiled-coil domain and two C-terminal zinc fingers. Two vertebrate paralogs exist, Tax1BP1 (also known as TXBP151 or T6BP) and Cocoa (also known as Calcoco1).

To test whether NDP52 is required for the formation of Nap1–ubiquitin complexes, we depleted the protein from 293ET cell lysates (Fig. 2c). Removing NDP52 inactivated the capacity of the lysate to facilitate binding of GST-ubiquitin to luciferase-Nap1, which demonstrates an essential role for NDP52 in the formation of Nap1–ubiquitin complexes. Next we titrated bacterially expressed NDP52 into reactions containing bacterially expressed Nap1 and ubiquitin, and found that NDP52 on its own was sufficient to mediate Nap1–ubiquitin complex formation (Fig. 2d). The bell-shaped binding curve predicts separate binding sites for Nap1 and ubiquitin in NDP52; at high concentrations of NDP52, this binding scheme would favor dimeric subcomplexes over trimeric Nap1–NDP52–ubiquitin complexes.

By mapping the Nap1 and ubiquitin binding sites in NDP52 we found that the SKICH domain (amino acids 1–127) and the zinc finger (amino acids 420–446) were required for Nap1 and ubiquitin binding, respectively (Supplementary Figs. 4 and 5). Binding of the zinc finger to ubiquitin is consistent with a recent report describing such activity for the zinc finger of the NDP52 paralog Tax1BP1 (ref. 31). We confirmed binding of Tax1BP1 to ubiquitin; however, Cocoa, despite harboring a related zinc finger and SKICH domain, bound neither ubiquitin nor Nap1 (Supplementary Figs. 6 and 7). We took advantage of the failure of Cocoa to bind Nap1 and introduced clustered point mutations into NDP52 based on sequence differences between NDP52 and Cocoa. Two of the resulting NDP52

Figure 2 NDP52, a ubiquitin-binding component of TBK1 complexes. (a) Flowthrough from nickel-agarose column, separated by SDS-PAGE and stained with Coomassie blue. (b) Amino acid sequence of NDP52. Red and underlining indicates peptides identified by mass spectrometry. (c,d) Normalized ratio between luciferase activity bound to beads and present in lysates. The indicated purified GST fusion proteins coupled to beads were incubated with bacterially expressed Nap1(1–85) fused to luciferase. Reactions were complemented with lysates from 293ET cells that had been depleted with the indicated (α -) antibodies (c, top). Immunoblot of lysates after depletion (c, bottom). Reactions were complemented with the indicated amounts of lysates from *E. coli* cultures expressing myelin basic protein (MBP) fused to NDP52 (d). (e) Lysates of 293ET cells were immunoprecipitated (IP) using the indicated antibodies or an isotype control. Lysates and precipitates were blotted (IB) for the presence of TBK1, IKK ϵ and IKK β . (f) Lysates of 293ET cells were immunoprecipitated using the indicated antibodies or an isotype control. Precipitates were blotted for the presence of TBK1 and NDP52. Fusion proteins used in Figure 2 are further characterized in Supplementary Figure 1. Data in panels c–f are representative of at least two independent experiments. Ub, ubiquitin; PCNA, proliferating cell nuclear antigen.



mutants, the G62E W63A double mutant and the D101A D102A E103A triple mutant, failed to interact with Nap1, which confirms our conclusion that NDP52 binds through its SKICH domain to Nap1 (Supplementary Fig. 4).

We then investigated whether endogenous kinase complexes contain NDP52. We found that NDP52 precipitated with TBK1 and IKK ϵ but not with IKK β , whereas the IKK β adaptor NEMO precipitated with IKK β but with neither TBK1 nor IKK ϵ (Fig. 2e). We also observed that endogenous Nap1 and Sintbad but not Tank precipitated with NDP52 (Fig. 2f). These findings demonstrate that distinct TBK1 complexes exist in cells and that NDP52 is specifically associated with those that contain Nap1 and/or Sintbad. Taken together, our biochemical analysis identifies NDP52 as a constitutive component of TBK1 complexes containing Nap1 and/or Sintbad, to which it is recruited through its SKICH domain. The ability of NDP52 to bind ubiquitin suggests that this protein may couple Nap1- or Sintbad-containing TBK1 complexes to ubiquitin-transduced signals.

NDP52 recruits TBK1 to ubiquitin-coated *S. Typhimurium*

Because Nap1 and Sintbad colocalized with ubiquitin-coated *S. Typhimurium*, we speculated that NDP52 may recruit complexes of TBK1 and Nap1 or Sintbad to such bacteria. Consistent with this hypothesis, in *S. Typhimurium*-infected HeLa cells bacteria coated in ubiquitin were positive for an NDP52-specific antiserum (Fig. 3a,b). In contrast, an antibody to Cocoa, the non-ubiquitin binding paralog of NDP52, stained cells diffusely and did not colocalize with bacteria.

Ubiquitin-coated *S. Typhimurium* are localized to a LAMP1-negative cell compartment, most likely the cytosol⁴. If NDP52 is the receptor for ubiquitin-coated bacteria, NDP52 should also be found in this LAMP1-negative cell compartment. Indeed, in HeLa cells infected with *S. Typhimurium*, NDP52-coated bacteria resided largely outside the LAMP1-positive compartment (Fig. 3c,d). Direct evidence that the detection of *S. Typhimurium* by NDP52 depends on its ubiquitin coat came from the observation that NDP52 required

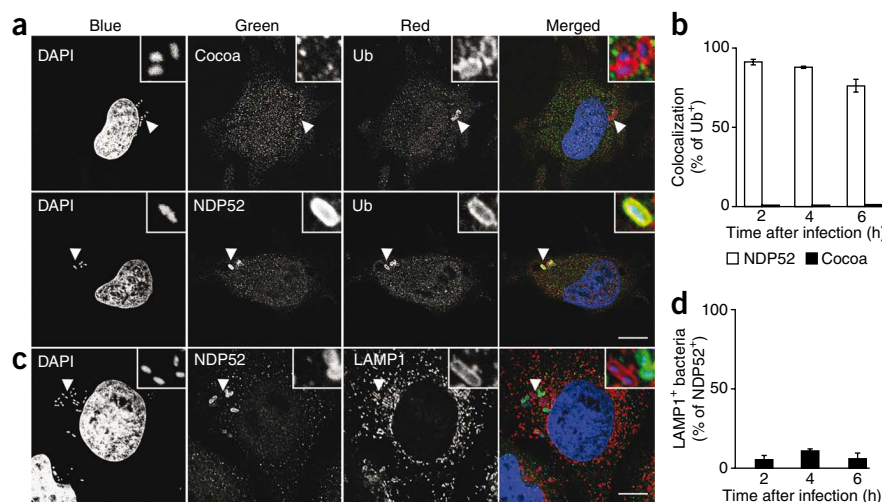


Figure 3 Ubiquitin-coated *S. Typhimurium* recruit NDP52. (a) Confocal micrographs of HeLa cells 2 h after infection with *S. Typhimurium*, stained with antibodies to Cocoa, NDP52 and ubiquitin (Ub). (b) Colocalization, at the indicated time points after infection, of ubiquitin-positive *S. Typhimurium* with NDP52 or Cocoa. (c) Confocal micrographs of HeLa cells 2 h after infection with *S. Typhimurium*, stained with antibodies to NDP52 and LAMP1. (d) Colocalization, at the indicated time points after infection, of NDP52-positive *S. Typhimurium* with LAMP1. DAPI, 4,6-diamidino-2-phenylindole. All data are representative of at least two independent experiments. Error bars, s.d.; three coverslips per experiment, >50 marker-positive cells evaluated per coverslip. Scale bars, 10 μ m; arrowheads, bacteria shown in insets.

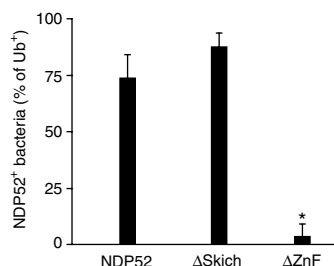


Figure 4 NDP52 senses the bacterial ubiquitin coat. Percentage of NDP52-positive *S. Typhimurium* among ubiquitin-coated bacteria, determined by microscopy. HeLa cells transduced with the indicated NDP52 domain-deletion mutants fused to green fluorescent protein were infected with *S. Typhimurium* and stained for ubiquitin 2 h after infection. ZnF, zinc finger domain. * $P < 0.01$, Student's *t*-test. Mean and s.d. of triplicate coverslips from two independent experiments; more than 50 ubiquitin-positive bacteria were evaluated per coverslip.

its zinc finger to colocalize with ubiquitin-coated *S. Typhimurium* (Fig. 4). In contrast, such colocalization did not depend on the SKICH domain of NDP52, demonstrating that the detection of ubiquitin-coated bacteria by NDP52 occurs independently of its association with Nap1, Sintbad or TBK1.

In agreement with our biochemical data, bacteria that stained positive for NDP52 colocalized with Nap1 or Sintbad but never with Tank (Fig. 5a). In addition, bacteria that stained for NDP52 also accumulated TBK1 (Fig. 5b). These data show that ubiquitin-coated *S. Typhimurium* recruits NDP52, Nap1, Sintbad and TBK1. Together with our biochemical analysis, these findings suggest that NDP52 acts as receptor subunit of TBK1 complexes and enables the detection of ubiquitin-coated bacteria. The accumulation of polyubiquitylated proteins and the recruitment of TBK1 are likely to happen after *S. Typhimurium* are released from their SCVs, which, in addition to the proposed homeostatic function for TBK1 in SCV maintenance⁶, suggests an active role for TBK1 in limiting the growth of *S. Typhimurium*.

NDP52 restricts growth of *S. Typhimurium*

To test whether NDP52 is required to restrict the growth of *S. Typhimurium* inside cells, we used RNA interference to deplete HeLa cells of NDP52, TBK1 or IKKε (Fig. 6a). Enhanced proliferation of *S. Typhimurium* occurred in cells lacking TBK1, as had been demonstrated before⁵, but not in cells lacking IKKε (Fig. 6b). Depletion of NDP52 with two different small interfering RNAs (siRNAs) also caused hyperproliferation of *S. Typhimurium*; the kinetics and magnitude of bacterial growth were similar between cells lacking TBK1 or NDP52 (Fig. 6c). Such restriction of *S. Typhimurium* growth by NDP52 was also observed in enterocytes, as demonstrated by the phenotype of HCT116 cells upon depletion of NDP52 with a lentiviral small hairpin RNA (Fig. 6d). Knockdown of NDP52 did not change the susceptibility of cells to infection with *S. Typhimurium*, as judged by the number of intracellular bacteria 2 h after infection (Fig. 6e). However, as early as 4 h after infection, the time at which bacteria began to proliferate in control cells, hyperproliferation was already detectable in NDP52-depleted cells. Notably, compared to control cells, a larger percentage of NDP52-depleted cells harbored ubiquitin-coated bacteria, particularly at 4 h after infection (Fig. 6f). We conclude that NDP52 is a cytosolic receptor of the innate immune system that recognizes and restricts the growth of ubiquitin-coated *S. Typhimurium*.

To test whether NDP52 would also restrict the growth of other bacterial species, we investigated two other human pathogens, the

Gram-negative bacterium *Shigella flexneri*, which causes dysentery, and the Gram-positive bacterium *Streptococcus pyogenes*, the etiological agent of diseases ranging from self-limiting pharyngitis to life-threatening necrotizing fasciitis. Both species can invade the cytosol of epithelial cells, but only *S. flexneri* is adapted to thrive in this compartment^{32,33}. A fraction of *S. pyogenes*, like *S. Typhimurium*, became coated with ubiquitin by 2 h after infection of HeLa cells and colocalized with NDP52 (Supplementary Fig. 8a). In contrast, *S. flexneri* did not colocalize with ubiquitin or NDP52 (data not shown). Consistent with their respective patterns of NDP52 recruitment, *S. pyogenes* grew more efficiently in cells depleted of NDP52, whereas NDP52 depletion had no effect on the proliferation of *S. flexneri* (Supplementary Fig. 8b,c). These data demonstrate that NDP52 can also protect cells against the attempt of a Gram-positive bacterium to colonize their cytosol. In contrast, *S. flexneri*, as one may have expected for a cytosol-dwelling pathogen, has found means to avoid the accumulation of polyubiquitylated proteins at its surface. It will be interesting to learn how *S. flexneri* escapes ubiquitin coating and whether NDP52 can restrict the growth of *S. flexneri* once that escape mechanism has been thwarted.

NDP52 delivers *S. Typhimurium* into autophagosomes

Next we investigated how NDP52 restricts the growth of *S. Typhimurium*. TBK1 has been suggested to control *S. Typhimurium* by limiting aquaporin-1 expression and maintaining SCV integrity⁶. However, only once *S. Typhimurium* are released from SCVs do they become ubiquitin coated and colocalize with NDP52 and TBK1. This suggests that NDP52 and TBK1 restrict bacterial proliferation in the cytosol. If this is the case, their depletion and the overexpression of aquaporin-1 should independently augment bacterial hyperproliferation. Indeed, HeLa cells overexpressing aquaporin-1 and depleted

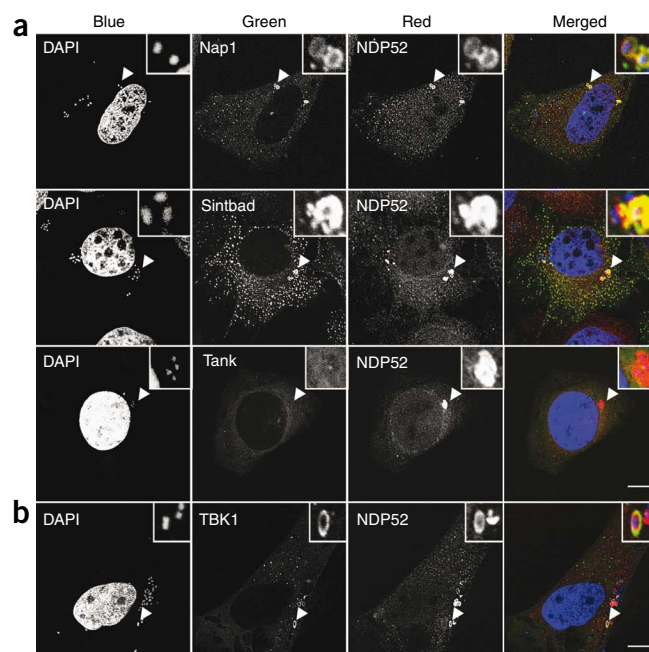
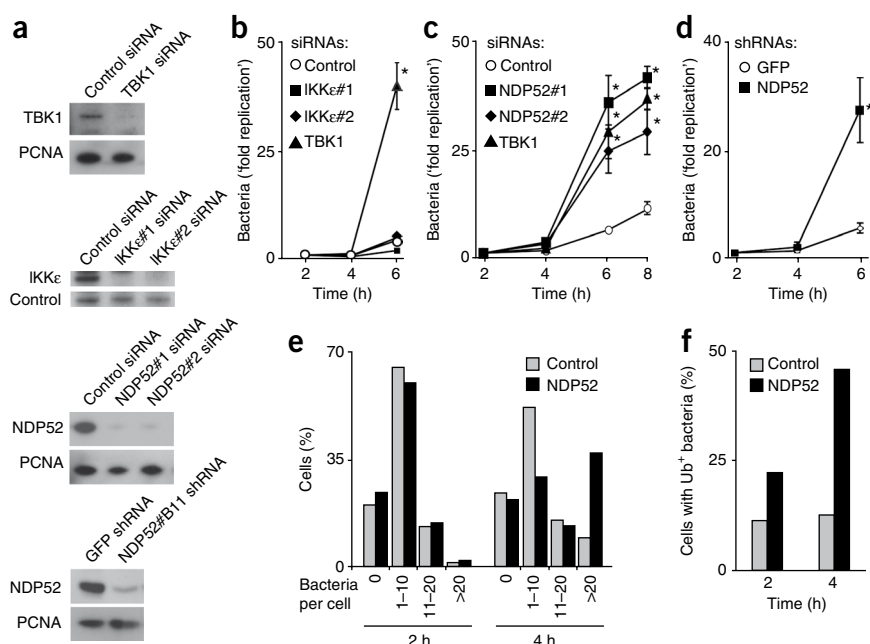


Figure 5 *S. Typhimurium* recruits NDP52-containing TBK1 complexes. (a,b) Confocal micrographs of HeLa cells expressing YFP-Nap1, YFP-Sintbad or YFP-Tank (a) or YFP-TBK1(K38M), a catalytically inactive mutant (b), stained with NDP52 antiserum 2 h after infection with *S. Typhimurium*. All data represent at least two independent experiments. DAPI, 4,6-diamidino-2-phenylindole. Scale bars, 10 μm; arrowheads, bacteria shown in insets.

Figure 6 NDP52 and TBK1 restrict growth of *S. Typhimurium*. **(a)** Lysates of cells transfected with the indicated siRNAs blotted for NDP52, TBK1, IKK ϵ and proliferating cell nuclear antigen (PCNA). Control, a nonspecific band detected by the IKK ϵ antibody. **(b,c)** Numbers of bacteria recovered from HeLa cells transfected with the indicated siRNAs and infected with *S. Typhimurium*. At the indicated time points after infection, cells were lysed and bacteria counted on the basis of their ability to form colonies on agar plates. Mean and s.d. of triplicate HeLa cultures and duplicate colony counts. **(d)** Numbers of bacteria recovered from HCT116 cells expressing the indicated shRNAs and infected with *S. Typhimurium*. At the indicated time points cells were lysed and bacteria counted by flow cytometry. Mean and s.d. of triplicate cultures. **(e)** HeLa cells transfected with the indicated siRNAs were infected with *S. Typhimurium* expressing green fluorescent protein (GFP). At the indicated time points after infection, cells were scored according to the number of bacteria they contained. **(f)** HeLa cells transfected with the indicated siRNAs were infected with *S. Typhimurium* expressing GFP. At the indicated time points after infection, cells were stained for ubiquitin and infected cells were scored if they contained ubiquitylated bacteria. All data represent at least two independent experiments. * $P < 0.05$, Student's t -test.



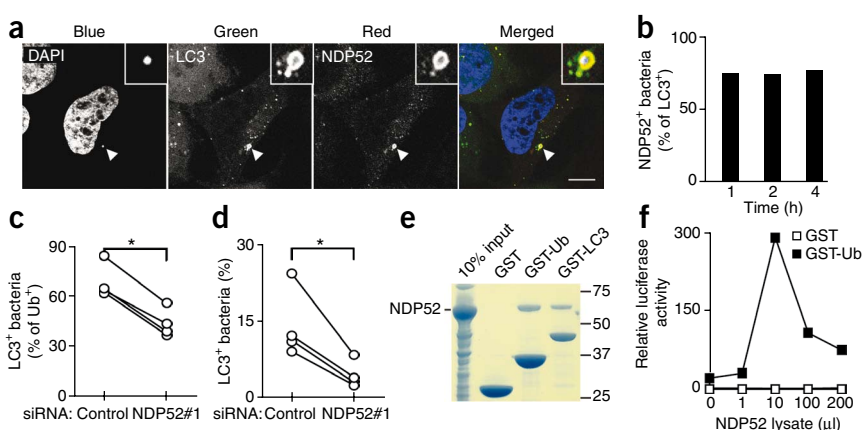
of NDP52 or TBK1 harbored more *S. Typhimurium* than cells either overexpressing aquaporin-1 or depleted of NDP52 or TBK1 (Supplementary Fig. 9).

Having established an aquaporin-1-independent function for NDP52 and TBK1, we tested whether the restriction of *S. Typhimurium* growth required macroautophagy, which has been suggested to contribute to innate immunity against cytosolic bacteria³⁴. In the following we will refer to this process simply as autophagy. We first tested whether NDP52- or ubiquitin-coated *S. Typhimurium* would be taken up into LC3-positive autophagosomes. We confirmed extensive colocalization of LC3 with ubiquitin-coated *S. Typhimurium*¹⁶ and observed similar accumulation of LC3 around NDP52-positive bacteria (Fig. 7a–d).

Knockdown of NDP52 decreased the percentage of ubiquitin-coated bacteria present in LC3-positive autophagosomes, as well

as the absolute number of *S. Typhimurium* that stained with LC3 (Fig. 7c,d). These results demonstrate that NDP52 is required for efficient autophagy of ubiquitin-coated *S. Typhimurium*. To test whether NDP52 is an autophagy receptor for ubiquitin-coated bacteria, we investigated whether it bound LC3. Purified GST-LC3 and GST-ubiquitin, but not GST alone, specifically precipitated NDP52 from lysates of NDP52-expressing *E. coli* (Fig. 7e), which demonstrates that NDP52 binds directly to LC3. If NDP52 functioned as an autophagy receptor, it might be expected to bind LC3 and ubiquitin simultaneously. Indeed, bacterially expressed NDP52, when titrated into reactions containing luciferase-LC3 and GST-ubiquitin-coated beads (a mimic of ubiquitin-coated bacteria), recruited LC3 to the ubiquitin-coated beads (Fig. 7f). The bell-shaped binding curve predicts separate binding sites for LC3 and ubiquitin in NDP52. We conclude

Figure 7 NDP52 binds LC3 and recruits ubiquitin-coated *S. Typhimurium* into autophagosomes. **(a–d)** Analysis of HeLa cells stably expressing green fluorescent protein-LC3, infected with *S. Typhimurium*. **(a)** Confocal micrographs of cells stained 1 h after infection with NDP52 antiserum. Scale bar, 10 μ m; arrowheads, bacteria shown in insets. **(b)** Colocalization of NDP52 with LC3-positive bacteria. **(c,d)** Counts of LC3-positive *S. Typhimurium* 1 h after infection in cells transfected with the indicated siRNAs. In **c**, cells were stained for ubiquitin (Ub); in **d**, red fluorescence protein (RFP)-expressing *S. Typhimurium* were used. Means of duplicate counts from four independent experiments; * $P < 0.05$, Student's t -test. **(e)** Binding of NDP52 to GST-LC3 and GST-ubiquitin. Beads carrying the indicated purified GST fusion proteins were incubated with lysates of *E. coli* expressing NDP52. Bound proteins were eluted with glutathione and stained with Coomassie blue after SDS-PAGE. **(f)** Normalized ratio of luciferase-LC3 binding to beads. The indicated purified GST proteins coupled to beads were incubated with bacterially expressed LC3 fused to luciferase and the indicated volumes of lysed *E. coli* expressing NDP52. Data in **a,b,e** and **f** are representative of at least two independent experiments.



that NDP52 is an autophagy receptor that detects ubiquitin-coated *S. Typhimurium*, and, by simultaneously binding LC3, directs the bacteria into autophagosomes. NDP52 thereby uses autophagy as an effector mechanism to restrict the growth of *S. Typhimurium*.

DISCUSSION

Mammalian cells limit bacterial growth inside endosomal and lysosomal compartments by, for example, lowering the pH, limiting the availability of ions, or attacking the invading pathogen with hydrolytic enzymes and reactive oxygen species. All of these defense mechanisms are incompatible with cytosolic function. In addition, the cytosol contains an abundance of nutrients, which raises the question of why only a few bacterial species have evolved to colonize it. Although it has been suggested that bacteria experimentally introduced into the cytosol may proliferate extensively³⁵, this result has been controversial³⁶, and under physiological circumstances innate immunity seems to prevent the colonization of the mammalian cytoplasm by most bacterial species. Bacterial growth is restricted by autophagy^{16,32,37–39} and by the bactericidal effects of ubiquitin⁴⁰ and, potentially, other proteins⁴¹. However, considering the complexity of cytosolic antiviral defenses, a variety of other mechanisms may exist.

In this work we defined the role of NDP52 in innate immunity against cytosolic bacteria and demonstrated that NDP52, together with two well established but previously unconnected phenomena—namely, the occurrence of ubiquitin-coated bacteria in the cytosol⁴ and the restriction of bacterial growth by TBK1 (ref. 5)—form the core of a newly identified cytosolic defense pathway in which NDP52 acts as autophagy receptor for ubiquitin-coated pathogens.

NDP52 shares with SQSTM1 (also called p62) and NBR1, the only other known ubiquitin-dependent autophagy receptors, the ability to bind LC3 and ubiquitylated cargo simultaneously^{42–45}. An important question for future investigations will be how individual autophagy receptors fulfill specific functions in cells. NDP52 and SQSTM1 may, for example, detect ubiquitin chains of different linkage types and, by recruiting distinct signaling molecules such as TBK1 and atypical protein kinase C^{46,47}, respectively, may determine the fate of the forming autophagosome and its cargo. Further questions emerging from our finding concern events upstream and downstream of the ubiquitin-sensing NDP52–Nap1/Sintbad–TBK1 complex. Identification of the E3 ubiquitin ligase responsible for the accumulation of ubiquitylated proteins at the bacterial surface will be critical, especially to determine whether this ligase acts as a new type of pattern recognition receptor. It will be equally interesting to identify the TBK1 substrate and to understand its role in autophagy, given that the enzymatic activity of TBK1 but not its canonical substrate, the transcription factor IRF3, is required for the restriction of bacterial growth⁵.

METHODS

Methods and any associated references are available in the online version of the paper at <http://www.nature.com/natureimmunology/>.

Accession codes. UCSD-Nature Signaling Gateway (<http://www.signaling-gateway.org/>): A001597.

Note: Supplementary information is available on the Nature Immunology website.

ACKNOWLEDGMENTS

We thank F. Begum and S.-Y. Peak-Chew for mass spectrometry, J. Kendrick-Jones (Medical Research Council Laboratory of Molecular Biology) for NDP52 antiserum, D. Holden (Imperial College London), C. Tang (Imperial College London), S. Sriskandan (Imperial College London) and C. Bryant (University of Cambridge) for bacterial strains and advice, A. Geerlof (European Molecular Biology Laboratory Heidelberg) for pETM plasmid, and D. Fearon, P. Lehner and D. Komander for comments.

AUTHOR CONTRIBUTIONS

T.L.M.T., G.R., S.B. and N.v.M. performed experiments and analyzed data. F.R. designed the overall research and wrote the manuscript.

Published online at <http://www.nature.com/natureimmunology/>.

Reprints and permissions information is available online at <http://npg.nature.com/reprintsandpermissions/>.

- Coburn, B., Grassl, G.A. & Finlay, B.B. *Salmonella*, the host and disease: a brief review. *Immunol. Cell Biol.* **85**, 112–118 (2007).
- Haraga, A., Ohlson, M.B. & Miller, S.I. *Salmonellae* interplay with host cells. *Nat. Rev. Microbiol.* **6**, 53–66 (2008).
- McGhie, E.J., Brawn, L.C., Hume, P.J., Humphreys, D. & Koronakis, V. *Salmonella* takes control: effector-driven manipulation of the host. *Curr. Opin. Microbiol.* **12**, 117–124 (2009).
- Perrin, A.J., Jiang, X., Birmingham, C.L., So, N.S. & Brumell, J.H. Recognition of bacteria in the cytosol of mammalian cells by the ubiquitin system. *Curr. Biol.* **14**, 806–811 (2004).
- Radtke, A.L., Delbridge, L.M., Balachandran, S., Barber, G.N. & O’Riordan, M.X. TBK1 protects vacuolar integrity during intracellular bacterial infection. *PLoS Pathog.* **3**, e29 (2007).
- Radtke, A.L. & O’Riordan, M.X. Homeostatic maintenance of pathogen-containing vacuoles requires TBK1-dependent regulation of aquaporin-1. *Cell. Microbiol.* **10**, 2197–2207 (2008).
- Fitzgerald, K.A. *et al.* IKKε and TBK1 are essential components of the IRF3 signaling pathway. *Nat. Immunol.* **4**, 491–496 (2003).
- Hemmi, H. *et al.* The roles of two IκB kinase-related kinases in lipopolysaccharide and double stranded RNA signaling and viral infection. *J. Exp. Med.* **199**, 1641–1650 (2004).
- McWhirter, S.M. *et al.* IFN-regulatory factor 3-dependent gene expression is defective in Tbk1-deficient mouse embryonic fibroblasts. *Proc. Natl. Acad. Sci. USA* **101**, 233–238 (2004).
- Ishii, K.J. *et al.* TANK-binding kinase-1 delineates innate and adaptive immune responses to DNA vaccines. *Nature* **451**, 725–729 (2008).
- Wu, C.J., Conze, D.B., Li, T., Srinivasula, S.M. & Ashwell, J.D. NEMO is a sensor of Lys 63-linked polyubiquitination and functions in NF-κB activation. *Nat. Cell Biol.* **8**, 398–406 (2006).
- Ea, C.K., Deng, L., Xia, Z.P., Pineda, G. & Chen, Z.J. Activation of IKK by TNFα requires site-specific ubiquitination of RIP1 and polyubiquitin binding by NEMO. *Mol. Cell* **22**, 245–257 (2006).
- Bloor, S. *et al.* Signal processing by its coil zipper domain activates IKK gamma. *Proc. Natl. Acad. Sci. USA* **105**, 1279–1284 (2008).
- Lo, Y.C. *et al.* Structural basis for recognition of diubiquitins by NEMO. *Mol. Cell* **33**, 602–615 (2009).
- Rahighi, S. *et al.* Specific recognition of linear ubiquitin chains by NEMO is important for NF-κB activation. *Cell* **136**, 1098–1109 (2009).
- Birmingham, C.L., Smith, A.C., Bakowski, M.A., Yoshimori, T. & Brumell, J.H. Autophagy controls *Salmonella* infection in response to damage to the *Salmonella*-containing vacuole. *J. Biol. Chem.* **281**, 11374–11383 (2006).
- Pomerantz, J.L. & Baltimore, D. NF-κB activation by a signaling complex containing TRAF2, TANK and TBK1, a novel IKK-related kinase. *EMBO J.* **18**, 6694–6704 (1999).
- Fujita, F. *et al.* Identification of NAP1, a regulatory subunit of IκB kinase-related kinases that potentiates NF-κB signaling. *Mol. Cell. Biol.* **23**, 7780–7793 (2003).
- Bouwmeester, T. *et al.* A physical and functional map of the human TNF-α/NF-κappa B signal transduction pathway. *Nat. Cell Biol.* **6**, 97–105 (2004).
- Ryzhakov, G. & Randow, F. SINTBAD, a novel component of innate antiviral immunity, shares a TBK1-binding domain with NAP1 and TANK. *EMBO J.* **26**, 3180–3190 (2007).
- Sasai, M. *et al.* Cutting Edge: NF-κB-activating kinase-associated protein 1 participates in TLR3/Toll-IL-1 homology domain-containing adapter molecule-1-mediated IFN regulatory factor 3 activation. *J. Immunol.* **174**, 27–30 (2005).
- Sasai, M. *et al.* NAK-associated protein 1 participates in both the TLR3 and the cytoplasmic pathways in type I IFN induction. *J. Immunol.* **177**, 8676–8683 (2006).
- Guo, B. & Cheng, G. Modulation of the interferon antiviral response by the TBK1/IKKi adaptor protein TANK. *J. Biol. Chem.* **282**, 11817–11826 (2007).
- Barrios-Rodiles, M. *et al.* High-throughput mapping of a dynamic signaling network in mammalian cells. *Science* **307**, 1621–1625 (2005).
- Zhao, T. *et al.* The NEMO adaptor bridges the nuclear factor-κB and interferon regulatory factor signaling pathways. *Nat. Immunol.* **8**, 592–600 (2007).
- Morton, S., Hesson, L., Pegg, M. & Cohen, P. Enhanced binding of TBK1 by an optineurin mutant that causes a familial form of primary open angle glaucoma. *FEBS Lett.* **582**, 997–1002 (2008).
- Koricho, F., Gieffers, C., Maul, G.G. & Frey, J. Molecular characterization of NDP52, a novel protein of the nuclear domain 10, which is redistributed upon virus infection and interferon treatment. *J. Cell Biol.* **130**, 1–13 (1995).
- Sternsdorf, T., Jensen, K., Zuchner, D. & Will, H. Cellular localization, expression, and structure of the nuclear dot protein 52. *J. Cell Biol.* **138**, 435–448 (1997).

29. Morriswood, B. *et al.* T6BP and NDP52 are myosin VI binding partners with potential roles in cytokine signalling and cell adhesion. *J. Cell Sci.* **120**, 2574–2585 (2007).
30. Gurung, R. *et al.* Identification of a novel domain in two mammalian inositol-polyphosphate 5-phosphatases that mediates membrane ruffle localization. The inositol 5-phosphatase skip localizes to the endoplasmic reticulum and translocates to membrane ruffles following epidermal growth factor stimulation. *J. Biol. Chem.* **278**, 11376–11385 (2003).
31. Iha, H. *et al.* Inflammatory cardiac valvulitis in TAX1BP1-deficient mice through selective NF- κ B activation. *EMBO J.* **27**, 629–641 (2008).
32. Nakagawa, I. *et al.* Autophagy defends cells against invading group A *Streptococcus*. *Science* **306**, 1037–1040 (2004).
33. Ray, K., Marteyn, B., Sansonetti, P.J. & Tang, C.M. Life on the inside: the intracellular lifestyle of cytosolic bacteria. *Nat. Rev. Microbiol.* **7**, 333–340 (2009).
34. Virgin, H.W. & Levine, B. Autophagy genes in immunity. *Nat. Immunol.* **10**, 461–470 (2009).
35. Bielecki, J., Youngman, P., Connelly, P. & Portnoy, D.A. *Bacillus subtilis* expressing a haemolysin gene from *Listeria monocytogenes* can grow in mammalian cells. *Nature* **345**, 175–176 (1990).
36. Goetz, M. *et al.* Microinjection and growth of bacteria in the cytosol of mammalian host cells. *Proc. Natl. Acad. Sci. USA* **98**, 12221–12226 (2001).
37. Ogawa, M. *et al.* Escape of intracellular *Shigella* from autophagy. *Science* **307**, 727–731 (2005).
38. Cadwell, K. *et al.* A key role for autophagy and the autophagy gene *Atg16l1* in mouse and human intestinal Paneth cells. *Nature* **456**, 259–263 (2008).
39. Yano, T. *et al.* Autophagic control of listeria through intracellular innate immune recognition in *Drosophila*. *Nat. Immunol.* **9**, 908–916 (2008).
40. Hiemstra, P.S., van den Barselaar, M.T., Roest, M., Nibbering, P.H. & van Furth, R. Ubiquicidin, a novel murine microbicidal protein present in the cytosolic fraction of macrophages. *J. Leukoc. Biol.* **66**, 423–428 (1999).
41. Beuzon, C.R., Salcedo, S.P. & Holden, D.W. Growth and killing of a *Salmonella enterica* serovar Typhimurium *sifA* mutant strain in the cytosol of different host cell lines. *Microbiology* **148**, 2705–2715 (2002).
42. Bjorkoy, G. *et al.* p62/SQSTM1 forms protein aggregates degraded by autophagy and has a protective effect on huntingtin-induced cell death. *J. Cell Biol.* **171**, 603–614 (2005).
43. Komatsu, M. *et al.* Homeostatic levels of p62 control cytoplasmic inclusion body formation in autophagy-deficient mice. *Cell* **131**, 1149–1163 (2007).
44. Pankiv, S. *et al.* p62/SQSTM1 binds directly to Atg8/LC3 to facilitate degradation of ubiquitinated protein aggregates by autophagy. *J. Biol. Chem.* **282**, 24131–24145 (2007).
45. Kirkin, V., Lamark, T., Johansen, T. & Dikic, I. NBR1 cooperates with p62 in selective autophagy of ubiquitinated targets. *Autophagy* **5**, 732–733 (2009).
46. Puls, A., Schmidt, S., Grawe, F. & Stabel, S. Interaction of protein kinase C zeta with ZIP, a novel protein kinase C-binding protein. *Proc. Natl. Acad. Sci. USA* **94**, 6191–6196 (1997).
47. Sanchez, P., De Carcer, G., Sandoval, I.V., Moscat, J. & Diaz-Meco, M.T. Localization of atypical protein kinase C isoforms into lysosome-targeted endosomes through interaction with p62. *Mol. Cell. Biol.* **18**, 3069–3080 (1998).

ONLINE METHODS

Antibodies. Clone or catalog numbers, if applicable, are given in parentheses. Antibodies to PCNA (PC10), TBK1 (sc9912), Tank (sc1997) and IκBβ (sc945) were from Santa Cruz; anti-NEMO (54/IKKγ) was from BD Pharmingen, anti-luciferase (MAB4400) from Chemicon, anti-NDP52 (N77920) from Transduction Laboratories, anti-ubiquitin (FK2) from Enzo Life Science, anti-aquaporin-1 (ab2219) from Millipore, anti-IKKε (ab7891) and anti-Lamp1 (H4A3) from Abcam and anti-Cocoa (A300-818A) from Bethyl Laboratories. HRP-conjugated reagents (anti-mouse P0447, anti-rabbit P0448, anti-goat P0449) were from Dabco, anti-Flag (M2) from Sigma, and Alexa-conjugated anti-mouse (A11031) and anti-rabbit (A10040) antisera from Invitrogen. The Sintbad antiserum has been described²⁰. The antiserum to Nap1 (256–393) expressed as an myelin basic protein (MBP) fusion protein was produced by Eurogentech. The antiserum to NDP52 was a gift from J. Kendrick-Jones.

Plasmids. M5P (ref. 48) or related plasmids were used to express proteins in mammalian cells. pETM plasmids were gifts from A. Geerloff. Genes encoding mouse Sintbad, Nap1, Tank, TBK1 and NEMO and human aquaporin-1, Optineurin, NDP52, Tax1BP1, Cocoa and LC3C were amplified by PCR or have been described^{13,15,20,49,50}. Mutations were generated by PCR and verified by sequencing. See **Supplementary Table 1** for primer sequences.

Cell culture. Human epithelial cell lines HeLa and HCT116 were obtained from the European Collection of Cell Cultures. A HeLa clone expressing GFP-LC3C was obtained by limiting dilution of retrovirally transduced cells.

Lumier assays.²⁴ Binding assays with pairs of putative interactors—one fused to luciferase and the other fused to GST—were performed as described previously²⁰.

Purification of NDP52 and peptide mass fingerprinting. Twelve liters of HeLa S3 cells were collected and lysed in 50 ml solution A (50 mM MES, pH 6.8, 100 mM NaCl, 10% (vol/vol) glycerol, 1 mM DTT) containing 0.2% (vol/vol) Triton X-100. Lysates were loaded onto a 10-ml Q Sepharose (GE Healthcare) column, washed with solution A and eluted with solution B (50 mM MES, pH 6.6, 500 mM NaCl, 10% (vol/vol) glycerol, 1 mM DTT). Fractions that supported binding of bacterially expressed luciferase-Nap1(1–85) to GST-ubiquitin were pooled and concentrated before being incubated with 500 μl of beads preloaded with His-GST-ubiquitin. Beads were washed with solution C (10 mM Tris-HCl, pH 7.4, 150 mM NaCl, 10% (vol/vol) glycerol, 1 mM DTT) and eluted twice with 5 ml solution C containing 10 mM glutathione. The eluate was incubated with 100 μl anti-Flag agarose preloaded with His-Flag-Nap1(1–158), and eluted twice with 150-μl volumes of solution C containing 160 μg/ml Flag peptide. Urea was added to a concentration of 5 M. Affinity ligands (His-GST-ubiquitin and His-Flag-Nap1(1–158)) were depleted twice with Ni-agarose. The supernatant was precipitated with cold acetone (1:4), resuspended in 25 μl SDS loading buffer and separated by PAGE. Coomassie-stained bands were excised and trypsin-digested before being analyzed by liquid chromatography/tandem mass spectrometry (LC-MS/MS). The extracted peptide mixture was partially dried and separated by nanoscale liquid chromatography (LC Packings) on a reverse-phase C18 column. The eluate was introduced directly into a Q-STAR hybrid tandem mass spectrometer (MDS Sciex). Spectra were searched against the NCBI nonredundant database with MASCOT MS/MS Ions (Matrixscience) search.

Immunoprecipitation and immunoblot. Postnuclear supernatants (5 min, 300g) from cells lysed in 0.5% (vol/vol) Triton X-100, 20 mM Tris HCl, pH 7.4, 150 mM NaCl and 1 mM EDTA were incubated with primary antibody and protein G–Sepharose. Immunoblots were performed as described²⁰.

Quantitative RT-PCR. cDNA was synthesized with oligo(dT) primers from a FirstChoice Human Total RNA Survey Panel (Ambion). Gene expression was measured on a Taqman machine (Applied Biosystems) by SybrGreen QPCR analysis (Applied Biosystems) using the following primers: 5′-ACC ATGGAGGAGACCATCAA-3′ and 5′-TCTTGGACGGAATTGGAAAG-3′ for *CALCOCO2*, encoding NDP52, and 5′CCTGGCACCCAGCACAAT-3′ and GCCGATCCACACGGAGTACT-3′ for *ACTB*, encoding β-actin (control).

RNA interference. Cells seeded in 24-well plates at 5×10^4 cells per well were transfected the next day with 40 pmol of siRNA (Invitrogen) using Lipofectamine2000 (Invitrogen). Alternatively, cells were transduced with pLKO.1-derived lentiviruses (Open Biosystems) expressing shRNAs. siRNAs and shRNAs targeted the following sequences: siTBK1, 5′-GACAGAAGUUGAUCACATT-3′; siNDP52#1 (*CALCOCO2*), 5′-UUCAGUUGAAGCAGCUCUGUCUCCC-3′; siNDP52#2, 5′-CCACCUCUUUCUCAGUUUACUGAA-3′; shNDP52#B11, 5′-GAGCUGCUUACUGAAAGAA-3′; siIKKε#1 (*IKBKE*), 5′-CAGGCAG UCCUGCACCACAUCUAUA-3′; siIKKε#2, 5′-GGAGUACCUGCAUCCCG ACAUGUAU-3′. The negative universal control with medium G+C content (Invitrogen) was used as a control.

Infections. *S. enterica* serovar Typhimurium (strain 12023) was grown overnight in LB broth (Fluka) and subcultured (1:33) for 3.5 h before infection. HeLa cells in 24-well plates were infected with 20 μl of such cultures for 15 min. After two PBS washes and an incubation with 100 μg/ml gentamicin for 1 h, cells were cultured in 20 μg/ml gentamicin. *S. flexneri* M90T was grown overnight in tryptic soy broth (TSB; Fluka) and subcultured (1:100) in TSB for 2 h before infection. Bacteria were washed in PBS and resuspended in warm IMDM. Bacterial suspensions (100 μl) were added to cells in 24-well plates. Plates were spun for 10 min at 670g to synchronize infection. After incubation at 37 °C for 30 min, cells were washed and cultured in 50 μg/ml gentamicin for the duration of the experiment. *S. pyogenes* (strain H293) was grown overnight in Todd-Hewitt broth (Fluka). Bacteria were washed in PBS and resuspended in five volumes of IMDM. HeLa cells in 24-well plates were infected with 12.5 μl of such resuspended bacteria, washed after 1 h twice with PBS and incubated with 100 μg/ml gentamicin for the next 2 h and with 20 μg/ml gentamicin thereafter. To count intracellular bacteria, cells from triplicate wells were lysed in 1 ml PBS containing 0.1% (vol/vol) Triton X-100 and plated in duplicate on TYE agar (*S. Typhimurium*), tryptic soy agar (*S. flexneri*) or Todd-Hewitt agar with 0.2% (wt/vol) yeast extract (*S. pyogenes*). To count *S. Typhimurium* by flow cytometry, bacteria in postnuclear supernatants (5 min, 300g) were fixed for 20 min with 4% (wt/vol) paraformaldehyde and resuspended in PBS containing a known number of caliBRITE-APC beads (BD Biosciences). Bacteria and beads were counted on a LSRII flow cytometer (BD Biosciences). Bacterial proliferation was assessed using the ratio of bacteria to beads.

Microscopy. HeLa cells grown and infected on glass cover slips were fixed in 4% (wt/vol) paraformaldehyde and quenched with PBS containing 1 M glycine and 0.1% (vol/vol) Triton X-100. Coverslips were blocked in PBTB (PBS, 0.1% (vol/vol) Triton X-100, 2% (wt/vol) BSA). Antibodies were applied in PBTB for 1 h. Cover slips were mounted using Vectashield medium with DAPI (Vector Laboratories). At least 100 events per slide were scored in quantitative assays. Confocal images were taken with a Nikon ×100, 1.4 numerical aperture objective on a Nikon Eclipse E800 microscope.

48. Randow, F. & Sale, J.E. Retroviral transduction of DT40. *Subcell. Biochem.* **40**, 383–386 (2006).

49. Randow, F. & Seed, B. Endoplasmic reticulum chaperone gp96 is required for innate immunity but not cell viability. *Nat. Cell Biol.* **3**, 891–896 (2001).

50. Krumbach, R., Bloor, S., Ryzhakov, G. & Randow, F. Somatic cell genetics for the study of NF-κB signaling in innate immunity. *Science Signaling* **1**, part 7 2008.